

Seismic refraction and downhole survey for characterization of shallow depth materials of Bam city, southeast of Iran

Riahi, M. A.^{1*}, Tabatabaei, S. H.², Beytollahi, A.³, Ghalandarzadeh, A.⁴, Talebian, M.⁵ and Fattahi, M.⁶

¹ Associate Professor, Earth Physics Department, Institute of Geophysics, University of Tehran, Iran

² Assistant Professor, Geotechnical Department, Building and Housing Research Center, Tehran, Iran

³ Assistant Professor, Geotechnical Department, Building and Housing Research Center, Tehran, Iran

⁴ Associate Professor, Civil engineering Department, University of Tehran, Iran

⁵ Assistant Professor, Geological Survey of Iran, Tehran, Iran

⁶ Assistant Professor, Earth Physics Department, Institute of Geophysics, University of Tehran, Iran

(Received: 21 Feb 2011, Accepted: 11 Oct 2011)

Abstract

Seismic refraction and downhole survey were employed to study dynamic characteristics of subsurface materials in Bam city, southeast of Iran. The data acquisition was performed at 160 P and S-wave refraction stations and 15 boreholes in the city. To derive velocity depth sections along these profiles as well as to perform downhole diagrams, SeisImager software was used. Based on the obtained values different maps consists of iso-depth, iso-velocity and iso-Poisson's ratio maps of city were prepared. The obtained results from the velocity variations of the P and S waves, three layers were identified. The first layer has low velocity, the second layer with medium velocity and the third layer has relatively high velocity values. The thickness of the first layer increases from the south west towards the north east of the study area while the thickness of second and third layers decreases from south west towards the north east of the study area, where in the south west of the region because of the thickening of the third layer, even using the far shot data of seismic measurement, the thickness of this layer was not detected. In the other word in the most part of the north east of the region, only two layers with low and medium velocity were determined. Attentive to the velocity distribution of the P and S wave velocity, the Poisson's ratio distribution as well as attenuation coefficient obtained for the identified layers of the area under investigation in the Bam city, it is concluded that the low velocity layer with high thickness and attenuation coefficient of the first layer can be attributed to be the cause of the strong motion vibration of the soil due to Bam earthquake on 26th December 2003 in the city.

Key words: Refraction, downhole, attenuation coefficients, Bam City

پی جویی های شکست مرزی و درون چاهی برای تعیین ویژگی های لایه های کم عمق

شهر بم، در جنوب شرقی ایران

محمدعلی ریاحی^۱، سیدهاشم طباطبائی^۲، علی بیت‌اللهی^۳، عباس قلندرزاده^۴، مرتضی طالبیان^۵ و مرتضی فتاحی^۶

^۱ دانشیار، گروه فیزیک زمین، مؤسسه ژئوفیزیک دانشگاه تهران، ایران

^۲ استادیار، بخش ژئوتکنیک، مرکز تحقیقات ساختمان و مسکن، تهران، ایران

^۳ استادیار، بخش ژئوتکنیک، مرکز تحقیقات ساختمان و مسکن، تهران، ایران

^۴ دانشیار، گروه مهندسی عمران، دانشکده فنی دانشگاه تهران، ایران

^۵ استادیار، پژوهشکده علوم زمین، سازمان زمین‌شناسی و معدنی، تهران، ایران

^۶ استادیار، گروه فیزیک زمین، مؤسسه ژئوفیزیک دانشگاه تهران، ایران

(دریافت: ۸۹/۱۲/۲، پذیرش نهایی: ۹۰/۷/۱۹)

چکیده

عملیات درون‌چاهی و شکست مرزی لرزه‌ای برای بررسی ویژگی‌های دینامیکی لایه‌های زیرسطحی شهر بم در جنوب شرقی ایران به انجام رسید. برداشت داده‌ها برای ۱۶۰ ایستگاه امواج شکست مرزی P و S و اندازه‌گیری امواج ذکر شده داخل ۱۵ گمانه در محدوده شهر به‌دست آمد.

برای تهیه مقاطع سرعت - عمق حاصل از نتایج لرزه شکست مرزی در محدوده مورد بررسی و همچنین تهیه نمودارهای درون‌چاهی از نرم‌افزار تصویرساز لرزه‌ای استفاده شده است. براساس مقادیر به‌دست آمده نقشه‌های هم‌عمق، هم‌سرعت و نسبت پواسون و ضریب تضعیف برای محدوده شهر تهیه شد.

با توجه به نتایج به‌دست آمده از تغییرات مقادیر سرعت امواج P و S، سه لایه لرزه‌ای تشخیص داده شد. به‌طوری‌که لایه اول دارای سرعت کم، لایه دوم دارای سرعت متوسط و لایه سوم دارای سرعت به‌نسبت زیادی بود. عمق لایه اول از جنوب غرب به سمت شمال شرقی محدوده مورد بررسی افزایش می‌یابد درحالی‌که عمق لایه‌های دوم و سوم از جنوب غرب به شمال شرق محدوده مورد بررسی کاهش پیدا می‌کند. در جنوب غرب محدوده مورد بررسی، به‌دلیل ضخیم بودن لایه سوم، حتی با استفاده از ثبت داده‌های شکست مرزی با دورافت زیاد نیز تعیین عمق این لایه میسر نشد. به‌عبارت‌دیگر در بیشتر قسمت‌های شمال شرقی محدوده، فقط دو لایه به‌ترتیب با سرعت‌های کم و متوسط تشخیص داده شدند. با توجه به توزیع مقادیر سرعت امواج P و S، توزیع نسبت پواسون و همچنین ضریب تضعیف به‌دست آمده برای لایه‌های مورد بررسی در شهر بم، این نتیجه حاصل شد که لایه اول که دارای سرعت کم، ضخامت زیاد و ضریب تضعیف زیاد است می‌تواند عامل جنبش نیرومند زمین ناشی از زلزله در تاریخ ۲۶ دسامبر ۲۰۰۳ در شهر بم باشد.

واژه‌های کلیدی: امواج شکست مرزی، ثبت درون‌چاهی، ضریب تضعیف، محدوده شهر بم

1 INTRODUCTION

The full potential of seismic methods in engineering investigations is yet to be realized. With investigative capabilities ranging from the detail of downhole measurement to the long traverses of studies of geological structure, the many available techniques can provide important information about the earth, its mass properties, its small-scale variations, and its anomalies of structure or content. The advantage of a seismic survey is that, it enables information to be obtained for large volumes of the earth that cannot be investigated by direct methods because of the costs involved. The applications of seismic refraction in studying of the dynamic characteristics of subsurface materials of underlying layers, e.g. the distribution and variations of thickness and velocity values in the ground, are still developing, but with great potential. These are still insufficiently or inappropriately used in engineering and the newer capabilities are not appreciated. There is a need for up-to-date guidance about how to apply seismic investigations. The seismic refraction method is often presented to engineering and

environmental professionals as an inexpensive and easily implemented geophysical method, particularly in comparison to seismic reflection methods. Several researchers (Chii and Osazuwa, 2010; Cardarelli et al., 2008; Dobecki and Upchurch, 2006; Nikrouz, 2005; Palmer, Nikrouz, and Spyrous, 2005; Cardarelli and de Nardis, 2001; Optim, 2001; Rucker, 2000) have attempted to present the full scope of modern seismic refraction applications to civil engineering projects.

In this article an attempt was made to apply seismic refraction and downhole survey to study dynamic characteristics of subsurface materials in Bam city. The city of Bam is located at the southwestern margin of the Dashte Lut desert, 50 km east of the Gowk fault. It is a flat area of a partially cemented alluvial fan system developed northward from Jebal Barez mountain ranges and feeds also from the north, by the hilly area built by Eocene volcanics and Paleogene pyroclastics (Figure 1, Askari et al., 2004). The only known structure of the Bam area was the east facing fault scarp of 15 to 20

meter high located 9 kilometer southeast of the town. The Mw 6.6 disastrous 26th of December 2003 earthquake which destroyed the city of Bam has no associated large co-seismic surface rupture zone (Fu, et al., 2004). Generally, three main subjects are involved in the present study: 1) Determination of soil layer velocities and thicknesses using the commercial software for interpretation. 2) Calculation of the Poisson's ratio of the layers. 3) Assessment of the first layer seismic quality factor and attenuation coefficient.

2 MATERIALS AND METHODS

2.1 DATA ACQUISITION

Seismic refraction data acquisition and downhole measurements was acquired in the Bam city to calculate velocity of the compressional wave, shear wave, Poisson's ratio as well as assessment of the first layer seismic quality factor and attenuation coefficient of the materials that forms the

subsurface layers in the Bam area. Distribution and design of the seismic profiles was based on providing a full coverage of the velocity distribution in the study area and to provide a possible correlation from geophysical engineering studies view point. Therefore, with respect to the rate of destruction in the Bam city due to Bam earthquake on 26th of December 2003, the boreholes as well as the seismic refraction profile locations have been selected. In this campaign 160 seismic refraction profiles consists of 80 profiles for the P-wave recording and 80 profiles for the S-wave recording were deployed, respectively. To record the down-going P and S waves and determination of the dynamic coefficients, 15 boreholes were selected and downhole measurements were acquired. In this context maximum depth of 12 boreholes was up to 30 meters while the depth of rest three boreholes were up to 60 meters (Figure 2).

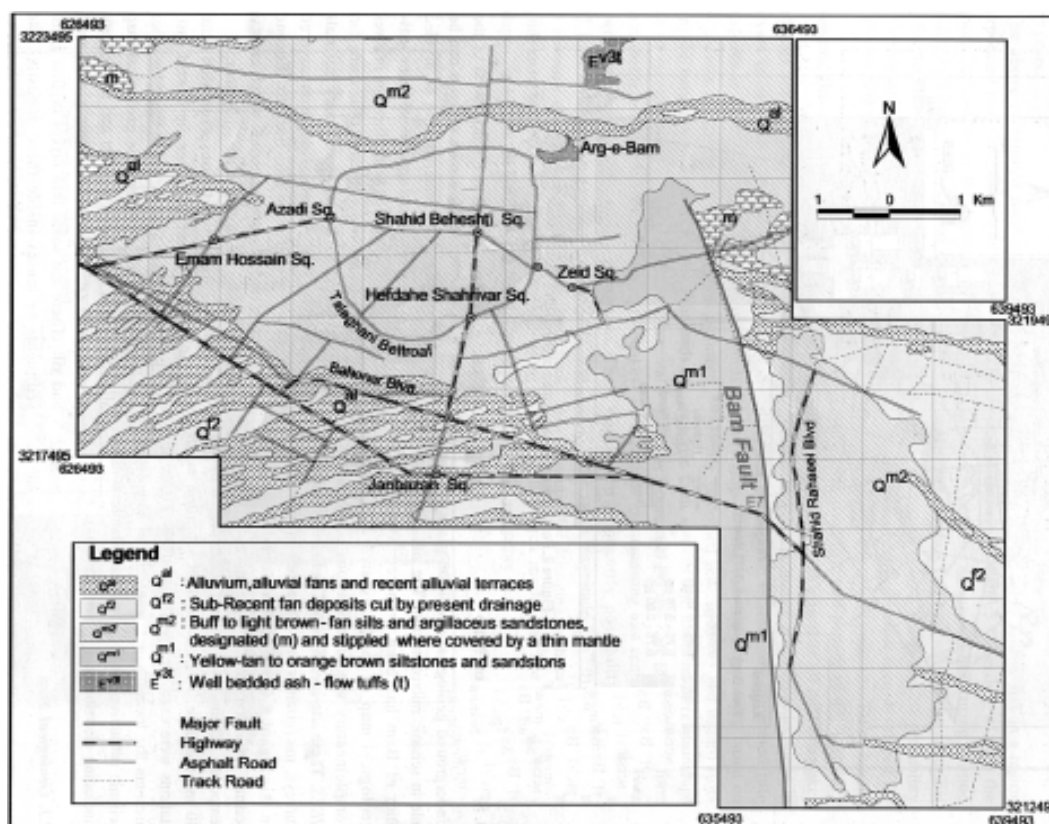


Figure 1. Distribution map of quaternary deposits in study area (Askari et al., 2004).

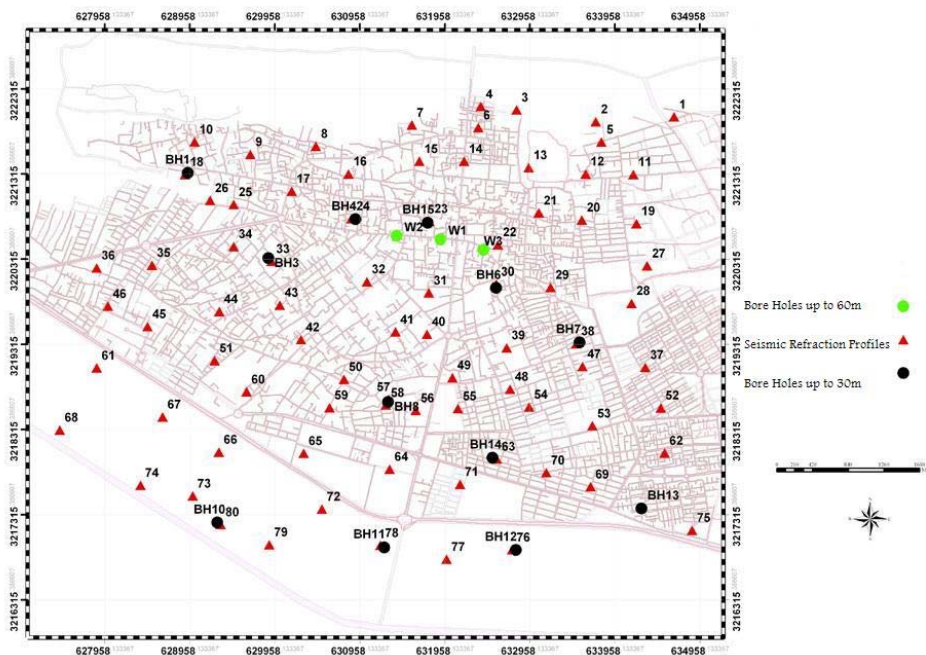


Figure 2. Location map of seismic refraction profiles shown with triangles, 15 boreholes shown with circles were selected for downhole measurements. In this context maximum depth of 12 boreholes shown with black circles was up to 30 meters while the depth of rest three boreholes shown with green circles were up to 60 meters.

In refraction data acquisition sledge hammer was used as seismic source and seven shots were performed along each profile. In this campaign, twenty four vertical geophones with 14 Hz natural frequency and twenty four horizontal geophones with 10 Hz natural frequency were applied. The data were recorded using ABEM Mark 6 instrument. Figure 3 shows the layout of the data acquisition.

In downhole data measurement, a three component probe comprising of two horizontal and one vertical geophone with natural frequency of 4.5 Hz and sampling rate of 100 ms were located at the required depth inside a borehole. Hammer was used as mechanical energy generating source. Hammer blows were applied on or on

opposite sides of a plank to generate P- and S-waves which reached the seismometer and were detected by the recorder. For shear waves, two records were taken at each particular depth which initially had reverse polarity. The wave reaching the seismogram is a direct wave; therefore, the energy source was positioned close to the borehole. The procedure was repeated at 1-m intervals by pulling up the probe. In order to verify the refraction results, downhole test was measured in boreholes. The results of down hole and refraction survey at one site are presented in Table 1. Results obtained from refraction were compared with the downhole data and it was shown that refraction data can be utilized for a reasonable estimation of the layer's thickness and velocities.

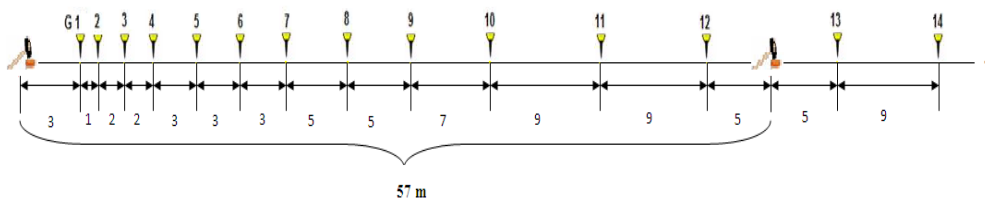


Figure 3. Shows the layout of refraction profile.

Table 1. Comparison between downhole and refraction data at BH12 location.

Refraction				Downhole					
Vp(m/s)	Vs(m/s)	Thickness(m)	Poisson's ratio	Depth	Interval		Average		Average Poisson's ratio
					Vp(m/s)	Vs(m/s)	Vp(m/s)	Vs(m/s)	
p1:630	s1:305	Z1:3	0.34	0	357	147	357	147	0.4
				1	416	202	416	202	0.35
				2	852	419	559	273	0.34
				3.2	1195	567	698	339	0.35
				3.6	1203	599	733	356	0.35
				4	948	457	750	364	0.35
				5	1064	539	797	389	0.34
p2:1180	s2:595	z2:22.8	0.32	6	1081	540	833	408	0.34
				7	1391	695	884	434	0.34
				8	1231	580	916	448	0.34
				9	1409	704	953	467	0.34
				10	1321	660	980	481	0.34
				11	1169	602	995	490	0.34
				12	1243	641	1012	500	0.34
				13	1244	642	1027	508	0.34
				14	1172	593	1036	514	0.34
				14.4	1139	595	1038	516	0.34
				p3:2000	s3:1120	z1+z:25.8	0.27	16	1316
18	1643	846	1104					550	0.34
20	1416	742	1129					565	0.33
22	1049	538	1121					562	0.33
24	1420	759	1141					575	0.33
27	1571	874	1177					597	0.32
30	2129	1196	1232					629	0.32
33	2295	1302	1286					660	0.32
36.5	1745	941	1320					679	0.3

3 DATA ANALYSIS

In the data analysis of refraction profiles, the following steps were processed:

1. Data monitoring: shot gather data were monitored and noisy traces were filtered out.
2. Selection of first arrivals: To improve the accuracy of acquired data, first arrivals of traces were selected and travel time curves were depicted.
3. Layering assignments: Layer assignments were made based o the dominant slope travel time curve segments. For this purpose each

layer attributed to more than three coherence arrival times.

4. In order to obtain velocity depth model, SeisImager software was used. This software accomplishes two modulus namely Pickwin and Plotrefa files. Travel time curve and layer assignment was performed with Pickwin module and ray-tracing approach was applied using Plotrefa module until an optimum model for each profile was achieved (Figure 4).

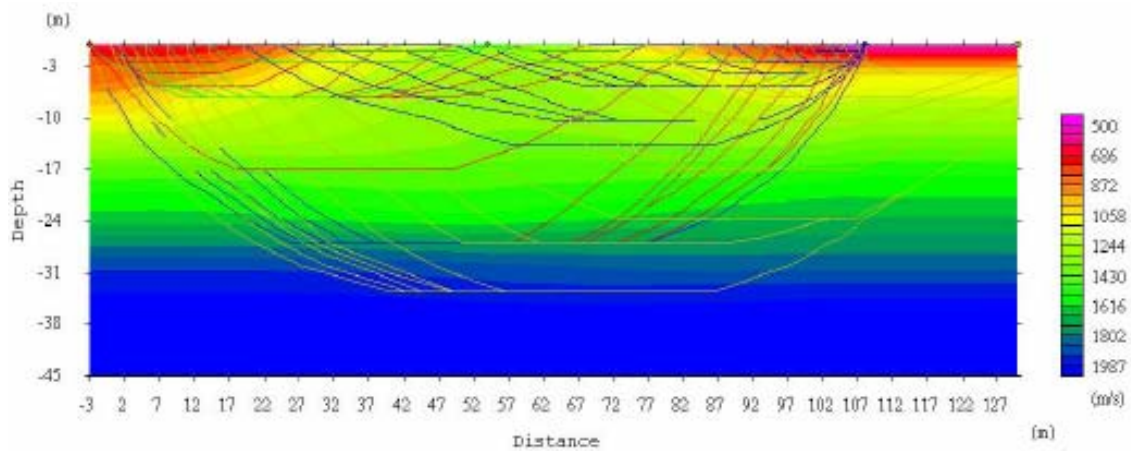


Figure 4. Shows the velocity depth model driven based on ray-tracing of refraction data.

4 RESULTS AND DISCUSSION

Based on the obtained results of the P and S wave velocity and thickness of the identified layers Poisson’s ratio in the Bam city were determined. Attentive to the obtained results from refraction and VSP data, the following items may be mentioned:

The compressional wave velocity distribution shown in Figure 5 indicates that the distribution of the P wave of the first low velocity layer in the north east and North West is varying between 360 to 500 m/s. The low velocity region can be seen in the central part of the region. Figure 6 shows the shear

wave velocity distribution for the first layer; shear wave velocity varies between 180 to 250 m/s in the north east, north west and central part of the study area. Comparison between the obtained P and S wave velocity values shows a good correlation. Calculated thickness for the first layer shows that the maximum thickness of this layer exists in the North East, North West and central part of the study area and it varies between 2 to 16 meters (Figure 7). Based on the obtained results the Poisson’s ratio of the first layer (Figure 8) varies from 0.3 to 0.37 which indicate that the first layer is unconsolidated.

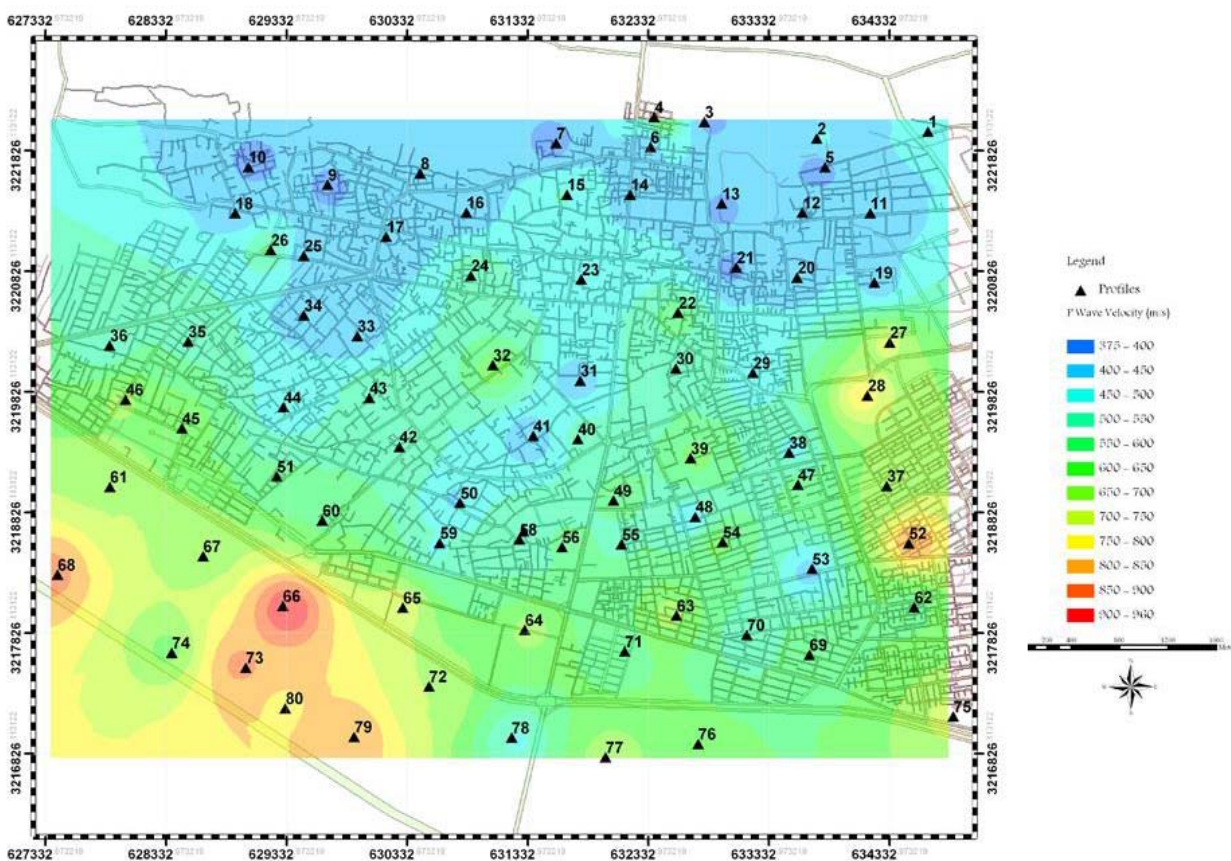


Figure 5. Shows distribution of the P- wave velocity obtained for the first layer. The velocity values in the North West towards North East is varying from 360 to 500 m/s. The velocity values in the central part from North West towards South East of the area is varying from 550 to 700 m/s. The velocity values in the South east part of the area are varying from 750 to 950 m/s.

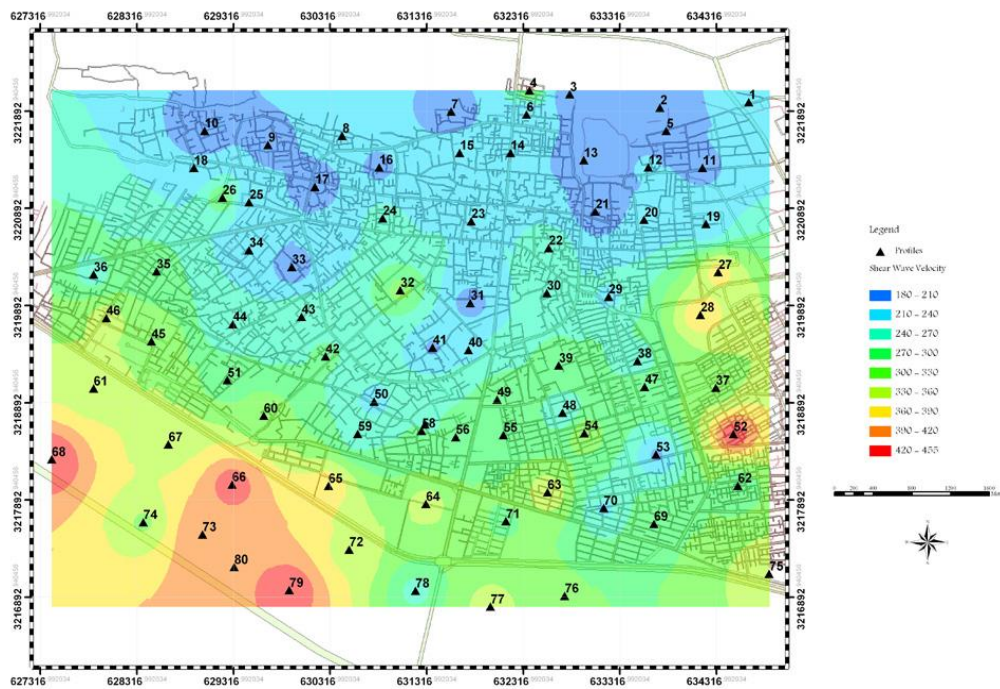


Figure 6. Shows distribution of the S- wave velocity obtained for the first layer. The velocity values in the North West towards North East is varying from 180 to 270 m/s. The velocity values in the central part from North West towards South East of the area is varying from 300 to 360 m/s. The velocity values in the South east part of the area are varying from 390 to 455 m/s. Comparison between the obtained P and S- wave velocity values shows a good correlation in distribution.

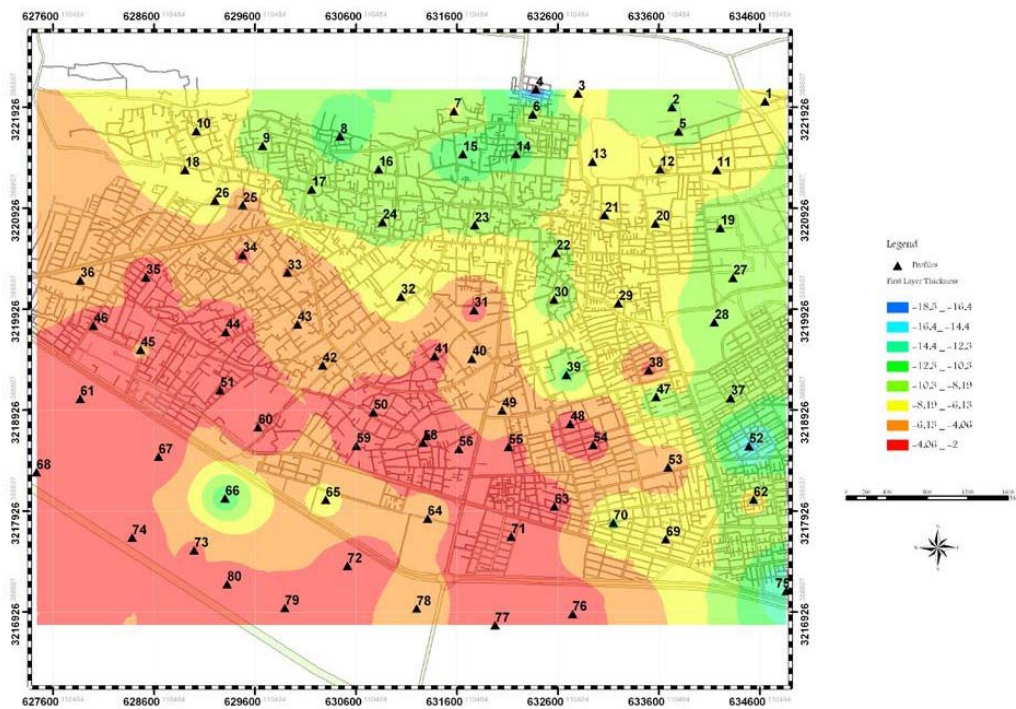


Figure 7. Shows distribution of the calculated thickness for the first layer. The thickness of this layer in the North West, North East towards South East is varying between 18.5 to 8.0 m. These values in the central part from North West to South East of the area is varying from 4.0 to 6.0 m. The values for thickness in the South East part of the area are varying from 4 to 2 m.

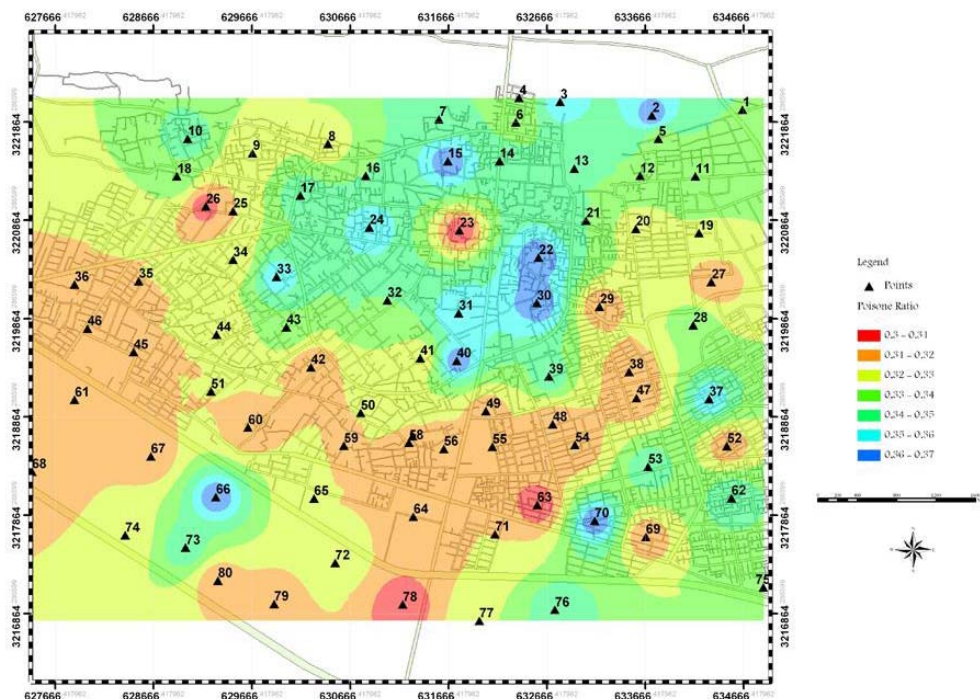


Figure 8. Shows the Poisson's ratio distribution of the first layer which varies from 0.3 to 0.37. The range of Poisson's ratio indicates that the first layer is consists of unconsolidated materials. The Poisson's ratio values of this layer in the North West, North East towards South East is varying from 0.37 to 0.34. These values in the central part from North West to South East of the area is varying between 0.33 to 0.32. The values for Poisson's ratio in the South East part of the area are varying from 0.32 to 0.3.

The obtained results shown in the Figure 9 indicates the compressional wave velocity value distribution and indicates that the distribution of the P wave of the second layer in the North East and South East is varying between 900 to 1200 m/s. The low velocity region can be seen in the South East towards central part of the region. Figure 10 shows the shear wave velocity distribution for the second layer, shear wave velocity varies between 180 to 250 m/s in the North East, South East and central part of the study area. Comparison between the obtained P and S wave velocity values shows a good correlation. Based on the obtained results the Poisson's ratio of the second layer (Figure 11) varies from 0.25 to 0.33 which indicate that the second layer is consisting of medium to consolidated materials (Tabatabaei et al., 2010). Calculated thickness for the second layer shows that the maximum thickness of the first and second layer exists in the North West towards South East direction. Figure 12 shows the P wave velocity distribution of the

third layer which its values varying in the study area. The result shows that in the Easter part of the Bam city the velocity value is grater than the other parts. Figure 13 shows the shear wave velocity distribution for the third layer and shows a good correlation with P wave velocity distribution. Based on the obtained P and S wave velocity values, the Poisson's ratio map was provided and has been presented in the Figure 14. Poisson's ratio for the third layer varies from 0.25 to 0.33. Therefore, the third layer may be classified into less, medium and high consolidated materials (Tabatabaei et al., 2010). To verify these results, fifteen boreholes were measured using downhole. P and S-wave velocity distribution versus depth, and their Poisson's ratio were calculated for each borehole, separately. Then, results obtained from refraction were compared to the VSP data and it was shown that refraction data can be utilized for a reasonable estimation of layer's thickness and velocities.

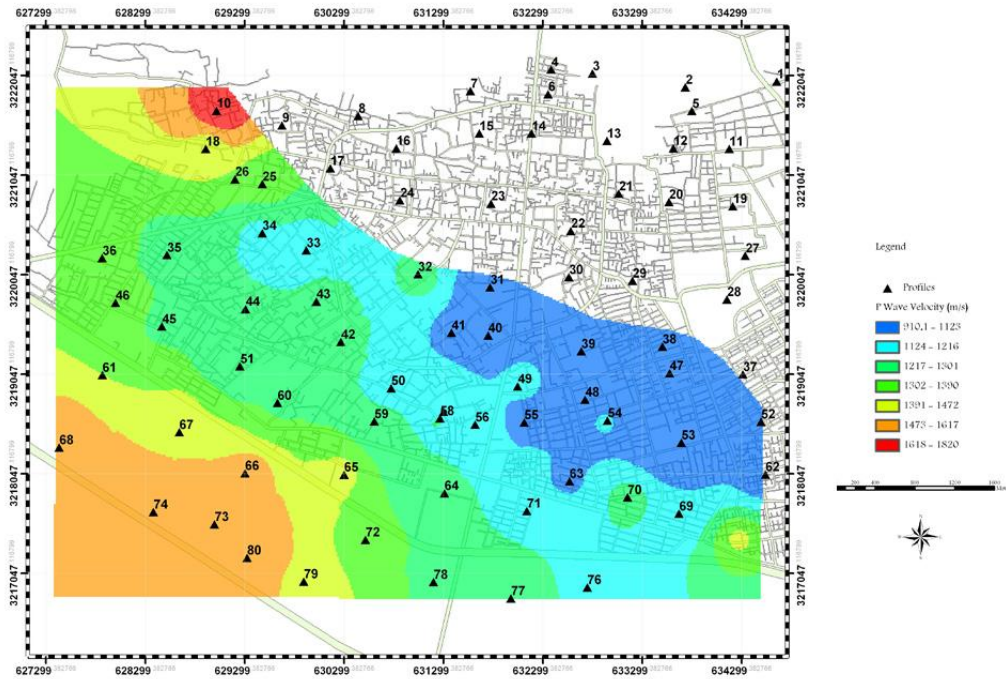


Figure 9. Shows distribution of the P- wave velocity obtained for the second layer. The velocity values in the central part of the study area from South East towards North West are varying from 900 to 1200 m/s. These values are varying from 1400 to 1800 m/s in the North East corner of the area. The velocity values in the South West part of the area are varying from 1400 to 1600 m/s. The blank area in this figure indicates that this layer was not detected under area of investigation.

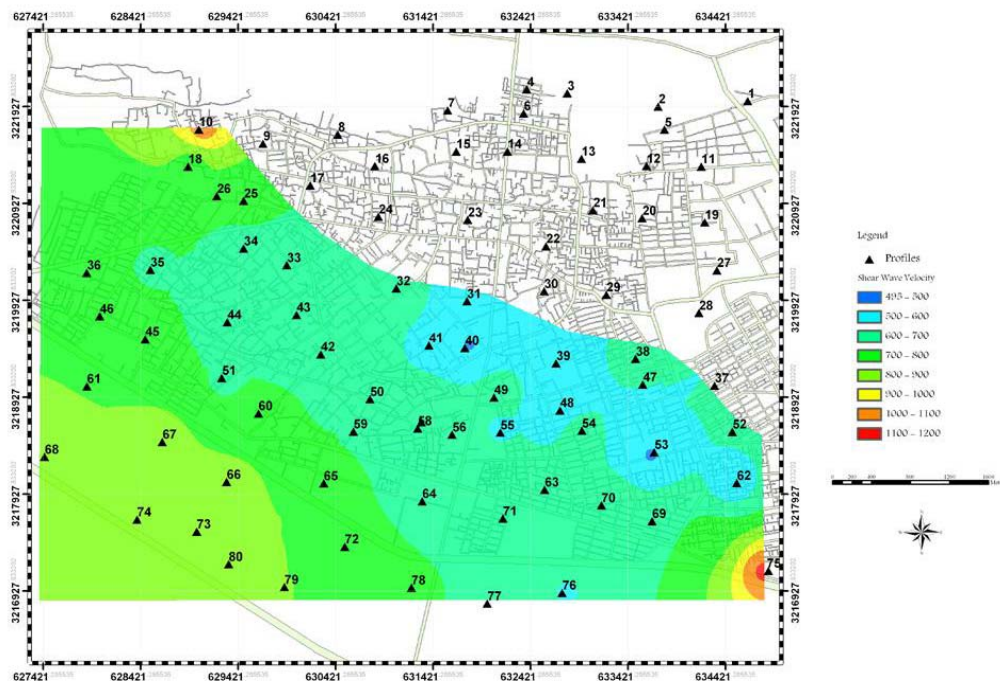


Figure 10. Shows distribution of the S-wave velocity obtained for the second layer. The velocity values in the central part of the study area from South East towards North West are varying from 500 to 700 m/s. The velocity values in the South West part of the area are varying from 700 to 800 m/s. The blank area in this figure indicates that this layer was not detected under area of investigation.

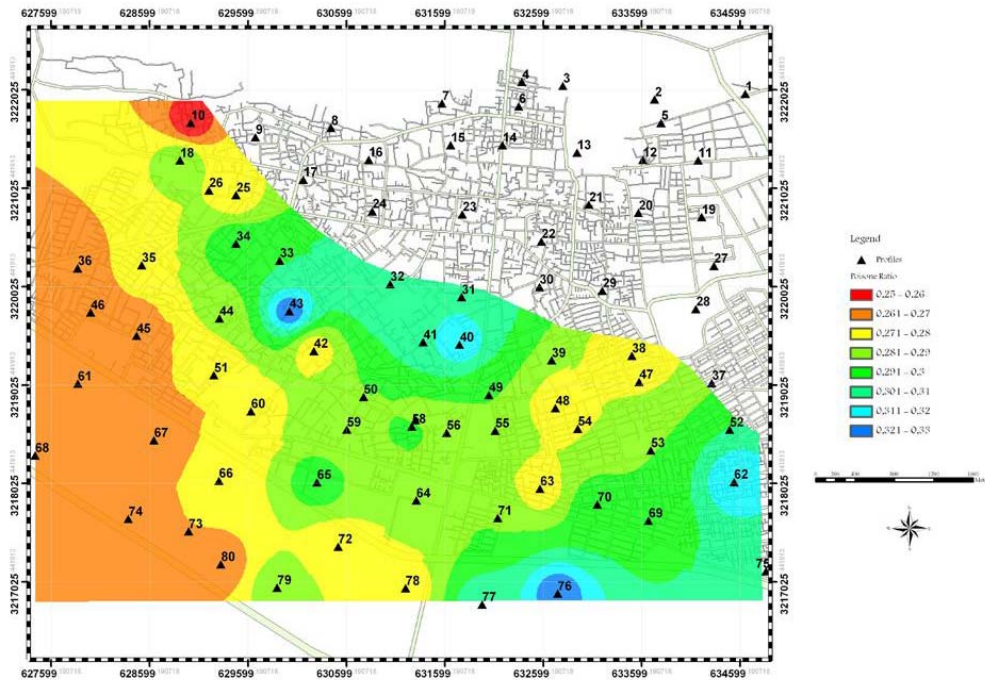


Figure 11. Shows the Poisson's ratio distribution of the second layer which varies from 0.25 to 0.33. The range of Poisson's ration indicates that the second layer is consists of medium to consolidated materials. The Poisson's ratio values of this layer in the North West corner to South West is varying from 0.25 to 0.27. These values in the central part from North West to South East direction of the area are varying from 0.28 to 0.31. The values for Poisson's ratio in the South East part of the area are varying from 0.32 to 0.33. The blank area in this figure indicates that this layer does not exist.

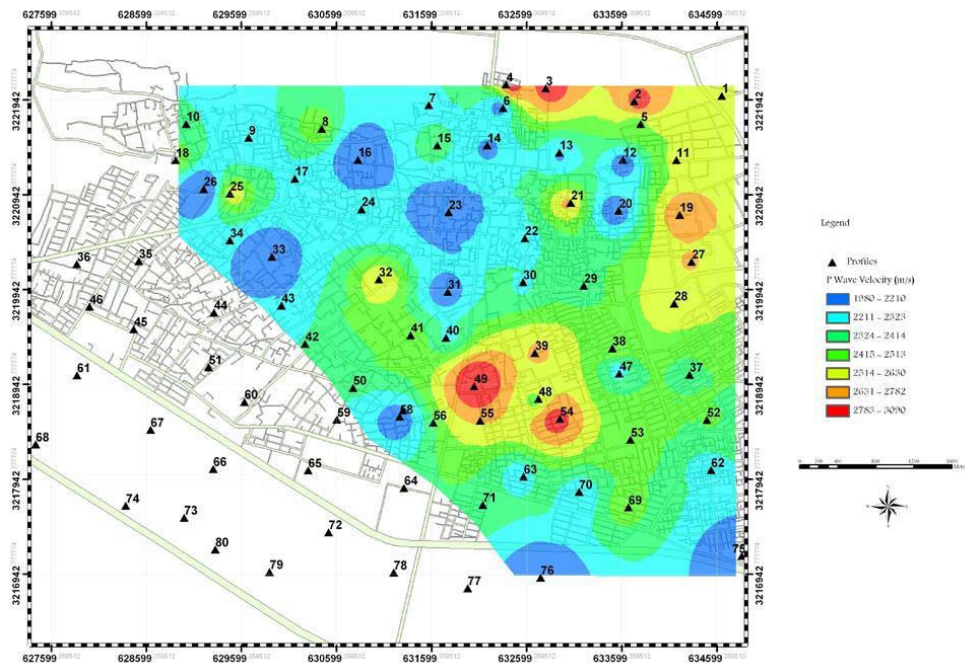


Figure 12. Shows the P- wave velocity distribution of the third layer which its values varying from 1980 to 3000 m/s in the area under investigation. The result shows that in the North East and center part of the Bam city the velocity value is greater than the other parts. The blank area in this figure indicates that, because of the thickening of the third layer even using the far shot data of seismic measurement, the thickness of this layer was not detected.

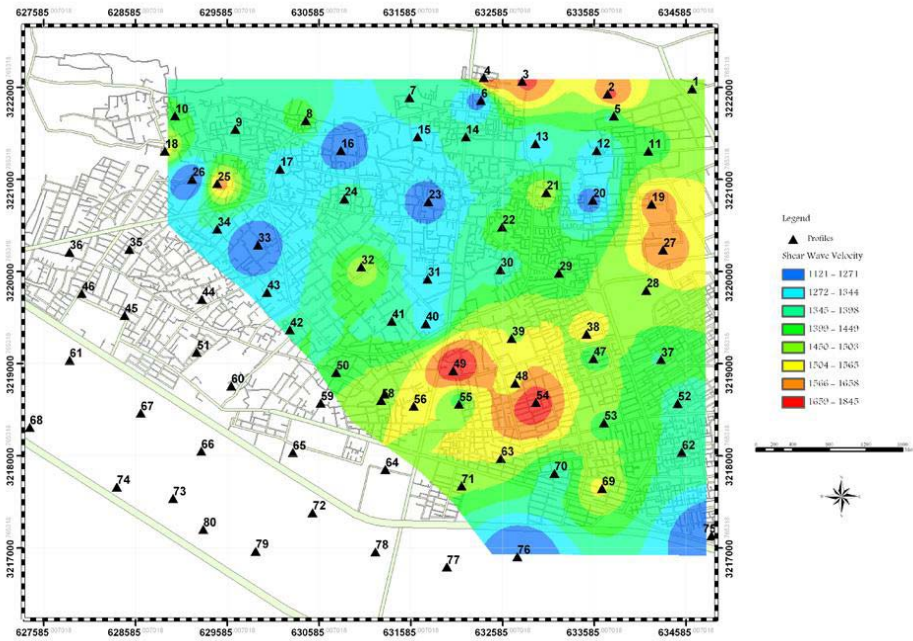


Figure 13. Shows the S- wave velocity distribution of the third layer which its values varying from 1100 to 1800 m/s in the area under investigation. The result shows that in the North East and center part of the Bam city the velocity value is grater than the other parts. The blank area in this figure indicates that, because of the thickening of the third layer even using the far shot data of seismic measurement, the thickness of this layer was not detected. This figure shows a good correlation with P- wave velocity distribution for third layer.

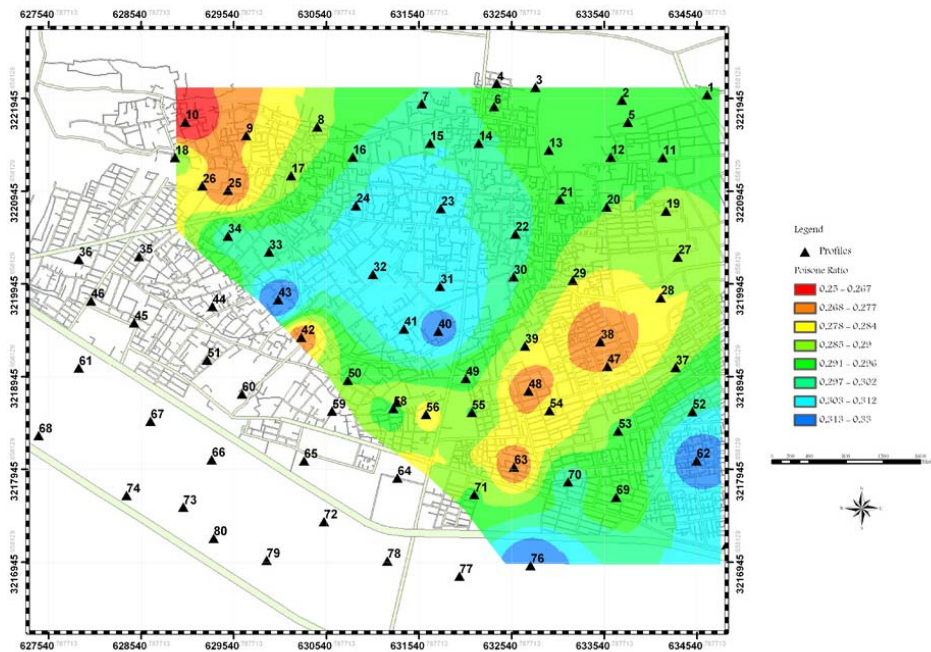


Figure 14. Shows the Poisson's ratio distribution of the third layer which varies from 0.23 to 0.33. The range of Poisson's ratiom indicates that the third layer is consists of medium to consolidated materials. The Poisson's ratio values of this layer in the North West and North East is varying from 0.23 to 0.29. These values in the central part from North West to South East of the area is varying between 0.28 to 0.33. The values for Poisson's ratio in the South East part of the area are varying from 0.3 to 0.33. The blank area in this figure indicates that, because of the thickening of the third layer even using the far shot data of seismic measurement, the thickness of this layer was not detected therefore, Poisson's ratio is not calculate.

In the geotechnical studies a map will be provided based on a shear wave velocity distribution of certain level, usually above 700 m/s which is so called seismic bedrock. This types of map usually used in related with seismic zonation of subsurface materials in the area under investigation. In this study, distribution of the seismic bedrock for the compressional wave equivalent with shear wave velocity of more than 700 m/s was provided (Tabatabaei et al., 2010). Figure 15 shows distribution of the compressional wave velocity varies from 1100 to 3100 m/s. Attentive to the result based on this figure, conclusion may be made that the P wave velocity distribution in the North East, South East and central part of the area under

investigation has grater values with respect to the South West and North West of the study area. Figure 16 shows the shear wave velocity distribution for the seismic bedrock which has a good correlation with the compressional velocity distribution. Thickness of the seismic bedrock varies from 6 to 29 meters and its distribution is provided in the Figure 17. The minimum and maximum thickness of the seismic bedrock exists in the area under investigation and show maximum depth at the central part of the Bam city. In the following, to have better insight about the obtained results, compressional and shear wave attenuation coefficient of the first layer has been prepared and studied.

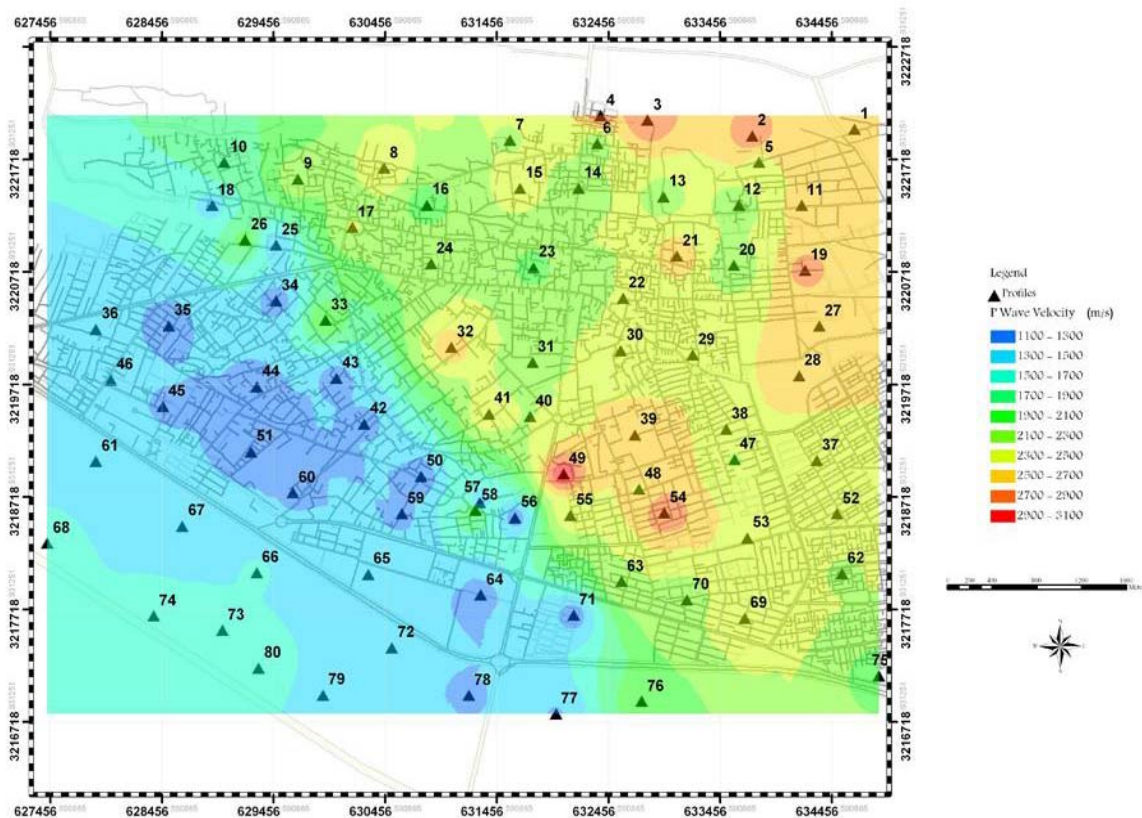


Figure 15. Based on geotechnical classifications, the shear wave velocities grater than 700 m/s is considered as seismic bedrock. This figure shows the distribution of seismic bedrock for the P-wave velocity equivalent with shear wave velocity of more than 700 m/s. In this map, the distribution of the P- wave velocity varies from 1100 to 3100 m/s. The velocity values are varying from 2300 to 3100 m/s in the North East towards South East. These values are varying from 1900 to 2300 in the central part with a North West and South East direction. The velocity value variation in the North West towards South West are varying from 1100 to 1700 m/s.

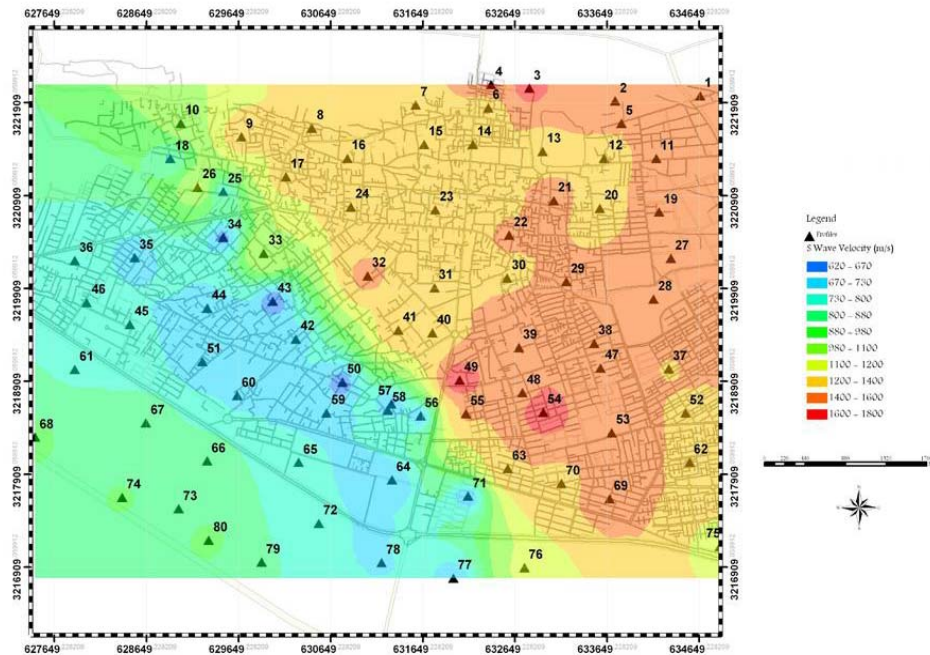


Figure 16. Based on geotechnical classifications, the shear wave velocities greater than 700 m/s is considered as seismic bedrock. This figure shows the distribution of seismic bedrock for the S-wave velocity. In this map, the distribution of the S-wave velocity varies from 600 to 1800 m/s. The velocity values are varying from 1200 to 1800 m/s in the North West and North East towards South East. These values are varying from 800 to 1100 in the central part with a North West and South East direction. The velocity value variation in the North West corner towards South West are varying from 600 to 800 m/s.

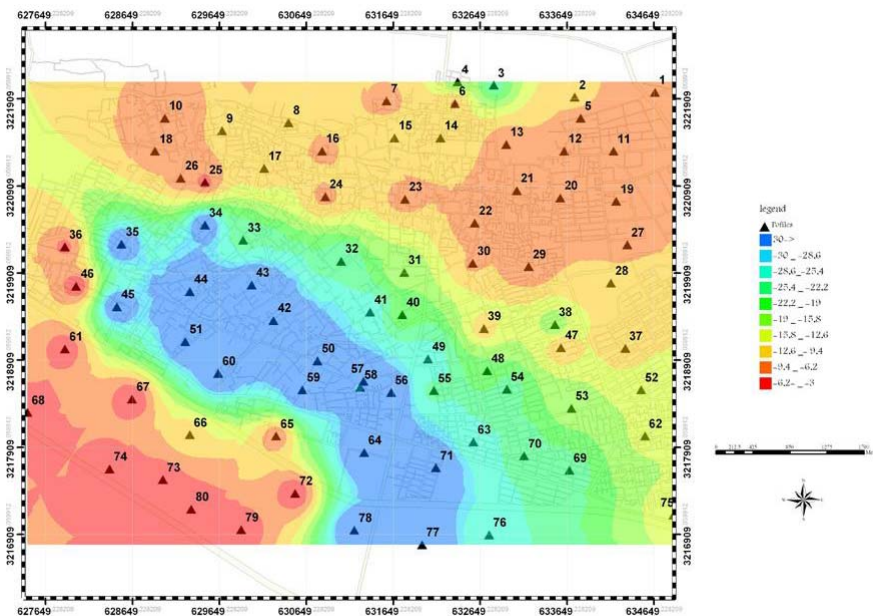


Figure 17. Based on geotechnical classifications, the shear wave velocities greater than 700 m/s is considered as seismic bedrock. This map shows thickness of the seismic bedrock variations in the area under investigation. The variation of thickness in the study area is from 3 to 29 meters. These values are varying from 3 to 12 m in the North West and North East towards South East. These values are varying from 19 to 29 m in the central part with a North West and South East direction. The thickness value variation in the North West corner towards South West are varying from 3 to 12 m. As can be seen, the maximum thickness of the seismic bedrock exists in the central part of the area under investigation. According to this map, subsurface materials in the study area are divided in three major seismic zones.

4.1 Q-ESTIMATION AND ATTENUATION STUDY

The seismic quality factor and attenuation coefficient are physically diagnostic of different types of rock materials. Much attention is now being paid to methods of determining Q directly from seismic data, particularly in shallow seismic surveys (Reynolds, 1997). Attenuation data have been traditionally obtained from laboratory measurements using ultrasonic transducers and through downhole experiments (e.g. Jones, 1986, and Klimentos and McCann, 1990). The amplitude of seismic wave decreases, the energy loss increases and the pulse width broadens (lengthens) with distance traveled as a result of four main processes: geometrical spreading, intrinsic attenuation (absorption), scattering and dispersion. There are more than ten methods dealing with the attenuation coefficient (α) and seismic quality factor (Q) measurements now in the literature (e.g., Tutuncu et al. 1994; Best, 1997; Prasad and Manghnani, 1997). Some of these methods are in time domain and others in frequency domain. These methods are pulse amplitude, rise time, pulse width, spectral ratio, amplitude decay, analytical signal, wavelet modeling, phase modeling, frequency modeling, spectral modeling and matching technique.

Wave propagation implies a variation of motion in space and time. Thus attenuation of wave motion can be considered in time or in space. For a given location wave motion is attenuated with time and, for a given time, it is attenuated with distance (Udias, 1999). The factor Q^{-1} is either represents the ratio of the decrease in amplitude during one period and the initial amplitude or represents the ratio of elastic energy ΔE dissipated during one cycle of harmonic motion of frequency ω and the maximum or mean energy E accumulated during the same cycle. Since the attenuation of body waves is measured from amplitudes at various distances. In most seismologic problems, it is assumed that there is no dissipation of energy in purely compressive or dilatational processes. Waters (1978) and also Udias (1999) review a

relationship between Q_p and Q_s which was derived assuming that there is no dissipation during a purely compressional cycle:

$$Q_p = (V_p/\text{constant})^2$$

$$Q_s = Q_p (4/3)(V_s/V_p)^2$$

Where V_p and V_s are compressional and shear wave velocities in feet per second, respectively and constant is approximately 10^3 (Hasse, et al., 2004). Based upon the above equation method Figures 18 and 19 are prepared. Figure 18 shows the attenuation coefficient of P-wave (Q_p^{-1}) distribution and indicates that the distribution of the attenuation coefficient P-wave of the first layer in the North East and North West is varying from 0.48 to 0.65. The central part of study area shows from North East towards South East from 0.32 to 0.43. The rest parts of region show attenuation coefficient variations from 0.1 to 0.26. Figure 19 shows the attenuation coefficient of S-wave (Q_s^{-1}) distribution and indicates that the distribution of the attenuation coefficient S-wave of the first layer in the North East and North West is varying from 1.76 to 2.12. The central part of study area shows from North East towards South East from 1.04 to 1.58. The rest parts of region show attenuation coefficient variations from 0.33 to 0.87. Comparison between the obtained P and S wave attenuation coefficient values showed a good correlation. Attenuation coefficients which calculated by equation method for the first layer shows that the maximum attenuation coefficient of the first layer is distributed in the North East, North West and center part towards South East of the Bam city, respectively. It is important to note that, the shear wave attenuation coefficient (Q_s^{-1}) shown in Figure 19 corresponds better with destructed zone of Bam city due to Bam earthquake on 26th December 2003 than attenuation coefficient of P-wave (Q_p^{-1}). The result in this section showed that attenuation coefficient is also an important dynamic characteristic for diagnostic of different types of rock materials.

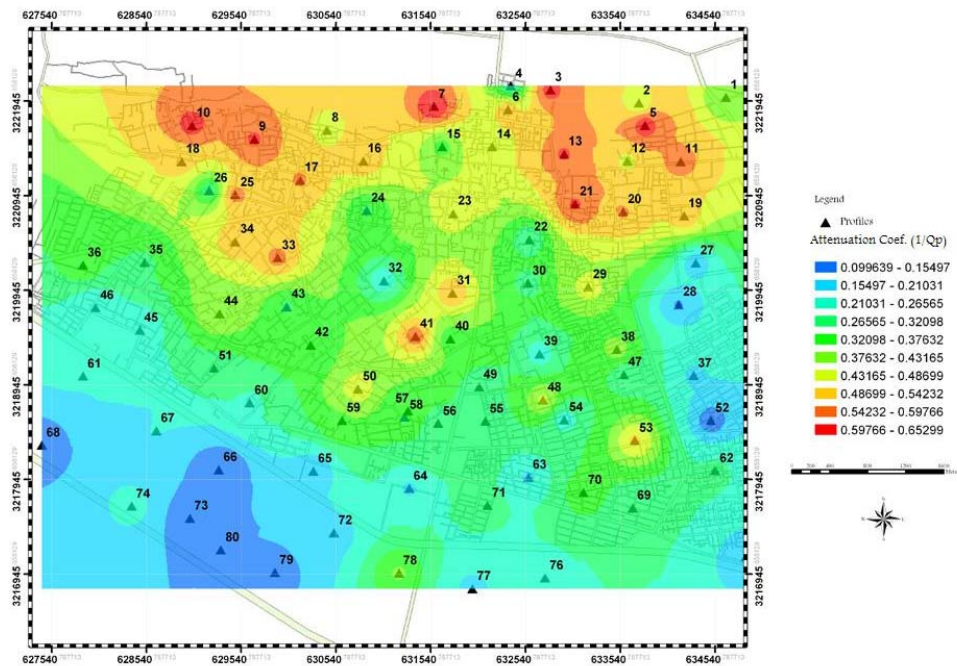


Figure 18. Shows the calculated attenuation coefficient values of P- wave (Q-1p) and its distribution in area under investigation. This map indicates that the distribution of the attenuation coefficient P- wave for the first layer in the North East and North West is varying from 0.48 to 0.65. The central part of study area shows attenuation coefficient variations in North East towards South East from 0.32 to 0.43. The rest parts of region show attenuation coefficient variations from 0.1 to 0.26, respectively.

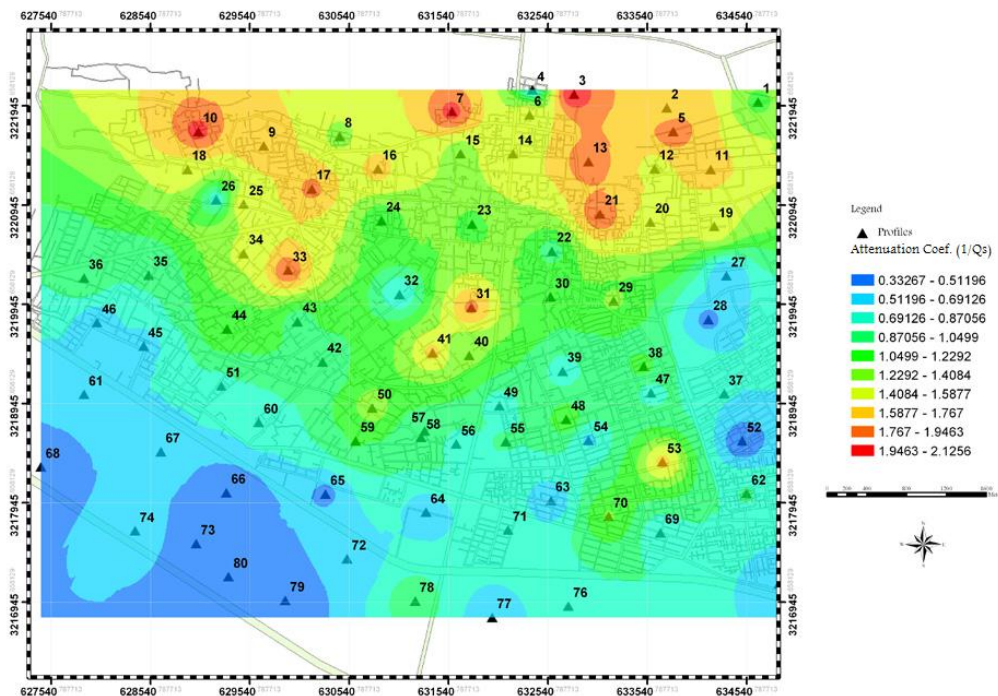


Figure 19. Shows the calculated attenuation coefficient values of S- wave (Q-1s) and its distribution for the first layer in area under investigation. This map indicates that the distribution of the attenuation coefficient S- wave for the first layer in the North East and North West is varying from 1.76 to 2.12. The central part of study area shows attenuation coefficient variations in North East towards South East from 1.04 to 1.58. The rest parts of region show attenuation coefficient variations from 0.33 to 0.87, respectively.

5 CONCLUSION

Three main subjects involved in the present paper are: (1) Determination of layers velocities and thicknesses by applying an accurate method of interpretation. It is concluded that lower seismic velocities and greater thicknesses than the surrounding parts characterize the North East and central part of the site under investigations. In this study velocity variations were obtained for the second layer varies between 900 to 1800 m/s for P-wave and 500 to 800 m/s for S-wave. Also velocity variations were obtained for the third layer varies between 1980 to 3000 m/s for P-wave and 1100 to 1800 m/s for S-wave. As can be seen there is no correlation between the obtained velocity values between the P and S velocity values for second and third layers.

(2) The dynamic properties of the first layer have been inferred and different competence scales have been applied for zonation of the foundation materials at the proposed site. The obtained Poisson's ratio values for the second layer and third layers from 0.25 to 0.33 provided the possibility of material classifications into less, medium and consolidated materials. These properties exhibit the occurrence of higher Poisson's ratio values in the North and central parts documenting again its lower material quality.

(3) The seismic quality factor and attenuation coefficient have been evaluated. These two parameters are physically diagnostic of the different types of soil and / or rock materials. This is because they reflect the differences in their anelastic properties. It is confirmed from this step that the North and central part of first layer posses lower values of the seismic quality factor with higher attenuation suggesting its lower material quality. This behavior is much pronounced in the attenuation coefficient of shear wave. The advantage of using seismic quality factor and attenuation coefficient of shear wave in differentiating the layer material quality over the quality factor and attenuation coefficient of compressional wave lies in taking into account the attenuation coefficient effect of seismic energy of compressional wave.

Based on the obtained results, the mapped area is divided into three zones of approximately the same dynamic properties of different parameters according to their calculated values, for which North East, center part and South West of Bam city consists of these zones respectively. Attentive to the velocity distribution of the P and S wave velocity, the Poisson's ratio distribution as well as attenuation coefficient obtained for the identified layers of the study area in the Bam city, it is concluded that the first layer with lower P and S wave velocities, high thickness and high attenuation coefficient overlaying on high velocity layer could amplify strong ground motion in destructive area due to Bam earthquake on 26th of December 2003 in the city.

ACKNOWLEDGEMENT

The first author greatly appreciates the support of Institute of Geophysics and University of Tehran which enabled the data acquisition. The authors are also grateful to Building and Housing Research Center, Tehran, Iran for cooperation on the seismic measurements. We appreciate the critical reading by arbitration committee and we will be acknowledging our gratitude for enlightening suggestion and insightful comments.

REFERENCES

- Askari, F., Azadi, A., DSavoodi, M., Ghayamghamian, M. R., Haghshenas, E., Hamzehloo, H., Jafari, M. K., Kamalian, M., Keshavarz, M., Ravanfar, O., Shafiee, A. and Sohrabi-Bidar, A., 2004, Preliminary seismic microzonation of Bam, JSEE Special Issue on Bam Earthquake, **5**, 69–81.
- Best, A. I., 1997, The effect of pressure on ultrasonic velocity and attenuation in near-surface sedimentary rocks, *Geophysical Prospecting*, **45**, 345-364.
- Dobrin, M. B. and Savit, C. H., 1988, *Introduction to geophysical prospecting*, John Wiley and Sons, Inc.
- Cardarelli, E., Fischanger, F. and Piro, S., 2008, *Integrated geophysical survey to*

- detect buried structures for archaeological prospecting, A case-history at Sabine Necropolis (Rome, Italy), *Near Surface Geophysics* **6**, 15–20.
- Cardarelli, E. and de Nardis, R., 2001, Seismic refraction, isotropic and anisotropic seismic tomography on an ancient monument, *Geophysical Prospecting* **49**, 228–240.
- Chii, E., Chii and Osazuwa, I. B., 2010, Seismic refraction tomography of the periphery of an artificial lake in the Precambrian basement complex of Northern, Nigeria *International Journal of the Physical Sciences* **5**(5), 421–431.
- Dobecki, T. L. and Upchurch, S. B., 2006, Geophysical applications to detect sinkholes and ground subsidence, *The Leading Edge* **25**, 336–341.
- Geological Survey of Iran (GSI), 1993, Geological Map of Iran scale 1: 100,000 series, sheet 7648Bam.
- Nazari, H., Parsons, B., Priestley, K., Talebian, M., Tatar, M., Walker, R. and Wright, T., 2006, Seismotectonic, rupture process, and earthquake-hazard aspects of the 2003 December 26 Bam, Iran, earthquake, *Geophys. J. Int.*, **133**, 390–406.
- Jannsen, D., Voss, J. and Theilen, F., 1985, Comparison of methods to determine Q in shallow marine sediments from vertical reflection seismograms, *Geophysical Prospecting*, **33**, 479–497.
- Jones, T. D., 1986, Pore fluids and frequency-dependent wave propagation in rocks: *Geophysics*, **51**, 1939–1953.
- Haase, A. B. and Stewart, R. R., 2004, Attenuation (Q) from VSP and Log Data: Ross Lake, Saskatchewan, CSEG National Convention.
- Klimentos, T. and McCann, C., 1990, Relationships among compressional wave attenuation, porosity, clay content, and permeability in sandstones, *Geophysics*, **55**, 998–1014.
- Lankston, R. W., 1988, High resolution refraction seismic methods, *Proc. of the Symp. on the Application of Geophys. to Engr. and Envr. Problems*, 349–387.
- Lankston, R. W., 1989, The seismic refraction method, A viable tool for mapping shallow targets into the 1990s, *Geophysics*, **54**, 1535–1542.
- Fu, B., Ninomiya, Y., Lei, X., Toda, S. and Awata, Y., 2004, Mapping active fault associated with the 2003 Mw 6.6 Bam (SE Iran) earthquake with ASTER 3D images, *Remote Sensing of Environment* **92**, 153–157.
- Prasad, M. and Manghnani, M. H., 1997, Effects of pore and differential pressure on compressional wave velocity and quality factor in Berea and Michigan sandstones, *Geophysics*, **62**, 1163–1176.
- Nikrouz, Ramin, 2005, Three-dimensional (3d) three-component (3c) shallow seismic refraction surveys across a shear zone associated with dryland salinity at the spicers creek catchment, New South Wales, Australia, dissertation (PhD), University of New South Wales, 488pages. Environmental Sciences, 2005.
- Optim, 2001, User's Manual SeisOptR@2DTM Version 2.8, Optim LLC, UNR-MS 174, 1664 N. Virginia St., Reno, Nevada.
- Palmer, D., Nikrouz, R. and Spyrous, A., 2005, Statics corrections for shallow seismic refraction data, *Exploration Geophysics*, **36**, 7–17.
- Reynolds, J. M., 1997, An introduction to applied and environmental geophysics, Baffins Lane, Chichester West Sussex PO 191 UD, England, 796 p.
- Riedel, M., Bellefleur, G., Dallimore, S. R., Taylor, A. and Wright, J. F., 2006, Amplitude and frequency anomalies in regional 3D seismic data surrounding the Mallik 5L-38 research site, Mackenzie Delta, Northwest Territories, Canada, *Geophysics*, **71**, 183–191.
- Robinson, E. S. and Coruh, C., 1988, Basic exploration geophysics: John Wiley and Sons, Inc.
- Rucker, M. L., 2000, Applying the Seismic Refraction Technique to Exploration for Transportation Facilities, in *Geophysics 2000, The First International Conference on the Application of Geophysical*

- Methodologies to Transportation Facilities and Infrastructure, St. Louis, Missouri, December 11-15, Paper 1-3.
- Sharma, P. V., 2002, Environmental and Engineering Geophysics, Cambridge University Press.
- Tabatabaei, S. H., Salamat, S., Ghalandarszadeh, A., Riahi, M. A., Beitollahi, A. and Talebian, M., 2010, Preparation of Engineering Geological Maps of Bam City Using Geophysical and Geotechnical Approach, Journal of Earthquake Engineering, 14: 4, 559 - 577.
- Tutunco, A. N., Podio, A. L. and Sharma, M. M., 1994, An experimental investigation of factors influencing compressional- and shear-wave velocities and attenuations in tight gas sandstones: Geophysics, **59**, 77-86.
- Udias, A., 1999, Principles of seismology, Cambridge University Press, page 260.
- Waters, K. H., 1978, Reflection Seismology, John Wiley and Sons, Inc., page 203.